Impact of Vanadium Doping on Magnetic Properties and Curie Temperature of HgTe Based on the Heisenberg Model and GGA Study

M. Baiboud[a,*], A. Labrag[a], M. Khenfouch[a,c], H. Charkaoui[a] and M. Bghour[b]

[a]*Laboratory of Materials, Electrical Systems, Energy and Environment (LM3SE), Materials and Energy Engineering Team, Faculty of Applied Sciences, Ibn Zohr University, Route Nationale 10, Cité Azrou, B.P. 32/S, 80000 Ait Melloul, Morocco*
[b]*Laboratory of Physics of Condensed Matter and Nano-Materials for Renewable Energies, Faculty of Sciences, Ibn Zohr University, Avenue Abdelkarim El Khattabi, B.P. 8106, 80000 Agadir, Morocco*
[c]*UNISA-UNESCO Africa Chair in Nanosciences-Nanotechnology, College of Graduate Studies, University of South Africa, Muckleneuk ridge, PO Box 392, Pretoria, South Africa*

Received: 10.06.2025 & Accepted: 16.01.2026

Doi: 10.12693/APhysPolA.149.115 *e-mail: deug.fsa@gmail.com

The *ab initio* study was performed using the generalized gradient approximations implemented in the CASTEP code to investigate the impact of vanadium doping on the electronic, optical, and magnetic properties of HgTe. The calculated lattice parameters of the compound under ambient conditions showed good agreement with experimental data. The pure HgTe compound is a semimetal, with the higher energy states of the valence band overlapping only the lower energy states of the conduction band. Doping with vanadium (V) induces ferromagnetism in the system, leading to a significant spin polarization of about 90% at the Fermi surface, making HgTe a potential candidate for spintronic applications. The Curie temperature (T_C) was estimated using mean field theory for doping concentrations of 12% and 24%. The double exchange is suggested as the most responsible interaction of ferromagnetism in the system. Optical calculations indicate enhanced absorption in the visible and infrared regions, suggesting its viability for optoelectronic device applications. These findings pave the way for the design of transition-metal-doped HgTe for the technological advancement of spintronics and photonics in the future.

topics: semimetal, ferromagnetism, $Hg_{1-x}V_xTe$, density functional theory (DFT)

1. Introduction

Ferromagnetic behavior is rarely observed in semiconductors due to the low carrier density. To enhance this behavior, a combination that integrates both semiconductor and magnetic properties, particularly within disordered systems, is recommended. For this purpose, dilute magnetic semiconductors (DMS) have been introduced [1–3]. These compounds are obtained by randomly introducing magnetic elements, such as transition metals or rare earth elements, into a non-magnetic semiconductor cationic matrix by substituting a fraction of its cations. In some cases, even non-magnetic elements may be used in the substation process [4–6]. The development of DMS as innovative materials with novel and interesting properties is expected to enable their applications in several areas of emerging technology [7–9].

Modifying the density of charge carriers affects several properties, with electronic and magnetic properties being of particular interest in this study. The main challenge is to obtain compounds exhibiting semimetallic behavior and ferromagnetic properties, with Curie temperature (T_C) exceeding room temperature, thereby enhancing their potential for spintronic device fabrication [10].

Mercury selenide (HgTe) does not exhibit a significant gap, nor does it show metallic behavior or act as a conventional semiconductor or insulator. It crystallizes in several phases, with the zinc blende structure being the most stable. HgTe has attracted considerable attention due to its unique properties,

making it a promising material for applications in optoelectronic and spintronic devices, as well as in thin-film transistors, light-emitting diodes, and electrochemical cells. It is also widely used in infrared detectors, adjustable lasers, and thermoelectric coolers, owing to its high electron mobility and elevated carrier concentration [11–14].

Research on V-doped HgTe remains in its early stages, and much of the relevant information must be inferred from studies on similar materials. Using vanadium as a dopant may introduce magnetism and enhance the electronic and optical properties of HgTe. Previous studies on Cr-doped GeO and GaN have shown room-temperature ferromagnetic behavior in dilute magnetic semiconductors, thereby broadening the scope for potential applications in optoelectronic and magnetic devices [15]. Furthermore, recent *ab initio* investigations have examined the effects of transition metal (TM) doping on the electronic, optical, and magnetic properties of various semiconductors. For instance, theoretical studies on $Cd_{1-x}TM_xTe$ (TM = V, Cr, Mn) have shown a semimetallic ferromagnetic behavior at high transition metal concentrations (x), making it relevant for spintronics applications [16]. At low concentrations, however, the doped CdTe remains insulating [17, 18]. Such findings support the hypothesis that vanadium doping in HgTe may lead to significant modifications of its intrinsic properties, which is necessary for effective use in electronics and spintronics.

This study aims to determine whether TM doping can meaningfully alter the fundamental properties of semiconductors. Specifically, the objective is to perform *ab initio* calculations to evaluate the impact of vanadium doping on the optical, electronic, and magneto–optical properties of HgTe. By analyzing the structural and electronic changes induced by doping, the work will assess the potential of V-doped HgTe for use in spintronic and optoelectronic applications, thus contributing to the broader understanding of TM-doped semiconductors.

2. Computational details

The calculations presented in this work, such as total and partial state density, band structure, magnetic moment, and other parameters, are obtained by applying the density functional theory (DFT) implemented in the CASTEP code and using the optimized Troullier–Martins–Goring (OTFG) pseudopotential [19]. The calculations were carried out within the generalized gradient approximation (GGA), without including spin–orbit coupling (SOC) effects [17, 18].

A $6 \times 6 \times 6$ Monkhorst–Pack k-point mesh was employed to ensure adequate sampling of the Brillouin zone, offering comprehensive coverage of the reciprocal space for precise calculations.

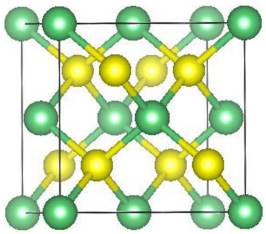

Fig. 1. Crystalline structure of the HgTe compound visualized using Vesta software.

Additionally, an energy cut-off of 500 eV was chosen to ensure both convergence and accuracy in the computational results. We showed that the primitive cell of HgTe is a zinc blende structure with space group $F\bar{4}3m$ and contains four atoms, including two atoms of mercury ($Z = 80$) and two atoms of tellurium ($Z = 52$). A $2 \times 1 \times 1$ supercell containing 16 atoms was employed to study the physical properties of V-doped HgTe. The material adopts a tetragonal structure with space group $P\bar{4}2m$ (no. 111).

The primary objective of these calculations is to replace one of the cationic sites in the semiconductor structure with a doping element — this time it will be the vanadium (V) atom. The introduction of this type of transition metal is intended to inject $3d$-TM impurities into the system. We have carried out a thorough study of the physical properties of the $Hg_{1-x}V_xTe$ compound. To assess the impact of vanadium substitution on magnetic properties, we used a supercell with a chemical composition of $Hg_7V_1Te_8$.

3. Results and discussions

3.1. Structural properties

The primitive cell of HgTe consists of two interpenetrating face-centered cubic (fcc) sublattices (see Fig. 1). Mercury atoms (with $Z = 80$) occupy the first sublattice, while tellurium atoms (with $Z = 52$) occupy the second. In this arrangement, Hg atoms are located at the $(0, 0, 0)$ position, and Te atoms are positioned at $(0.25, 0.25, 0.25)$. The experimental lattice parameter for HgTe is reported to be 6.46 Å [20].

To study the structural stability and determine the equilibrium properties of the material, the total energy as a function of volume is fitted using the third Birch–Murnaghan equation of state [21]

$$E = E_0 + \frac{9V_0B_0}{16}\left\{\left[\left(\frac{V_0}{V}\right)^{\frac{2}{3}} - 1\right]^3 B_0' + \left[\left(\frac{V_0}{V}\right)^{\frac{2}{3}} - 1\right]^2 \left[6 - 4\left(\frac{V_0}{V}\right)^{\frac{2}{3}}\right]\right\}. \quad (1)$$

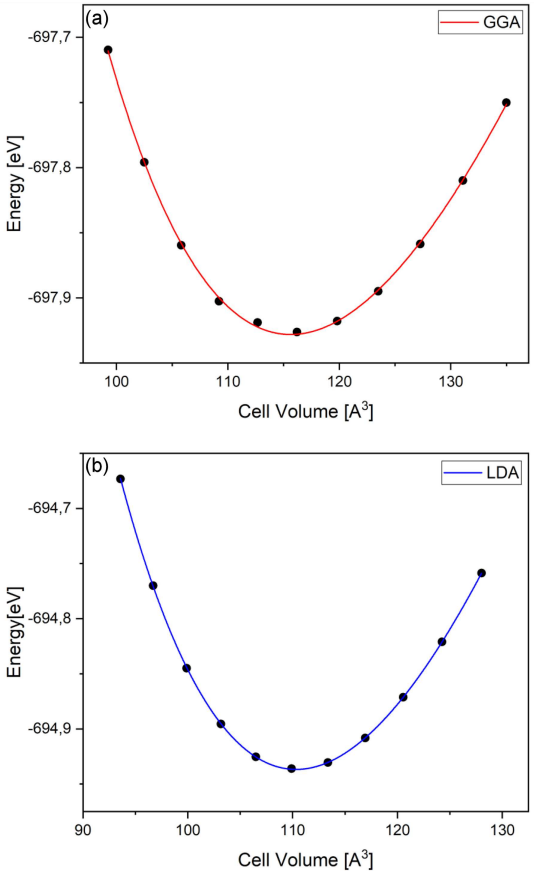

Fig. 2. Total energy versus cell volume of HgTe calculated using (a) GGA-PBE and (b) LDA.

In Fig. 2, the total energy as a function of unit cell volume for HgTe is presented, calculated using the generalized gradient approximation with the Perdew–Burke–Ernzerhof (GGA-PBE) and the local density approximation (LDA).

It was found that the results obtained using LDA differ significantly from other results, particularly for the lattice parameter a. The LDA approach underestimates this parameter by 0.07 Å compared to the experimental value. This discrepancy is in agreement with previous studies [22], which have also reported that LDA tends to underestimate the lattice constants due to its overbinding effect. In contrast, the results obtained using the generalized gradient approximation with the Perdew–Burke–Ernzerhof (GGA-PBE) functional are in good agreement with both experimental values and previous findings, as shown in Table I (see also [20–23]). The GGA-PBE method has been shown to provide a more accurate description of the structural properties of HgTe and related semiconductors in similar studies [24, 25]. Given this discrepancy, we opted to use the GGA-PBE method for calculating the other properties of HgTe, as it ensures greater accuracy and reliability, bringing our results into closer alignment with experimental data and other theoretical predictions.

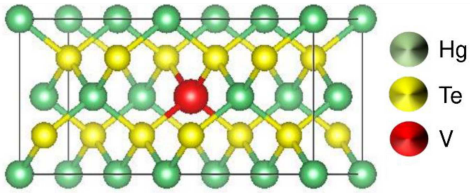

Fig. 3. Structure of the doping system Hg_7VTe_8.

TABLE I

Lattice parameter calculated using both GGA and LDA; our results compared with other results.

	Lattice parameter a
Present work (GGA)	6.50 Å
Present work (LDA)	6.39 Å
Experimental value	6.46 Å [23]
Other calculations (GGA)	6.41 Å [21], 6.664 Å [22]
Other calculations (LDA)	6.47 Å [20]

To investigate the impact of V substitution on the physical properties of the system, a supercell containing 16 atoms in total was used, corresponding to the chemical composition Hg_7VTe_8. As illustrated in Fig. 3, this supercell provides a representative model of our compound. A doping concentration of $x = 0.125$ was realized by substituting a mercury (Hg) with a vanadium (V) at the site of the HgTe supercell shown in Fig. 3. As a result of this substitution, the structure becomes tetragonal and crystallizes in the space group $P\bar{4}2m$ (no. 111).

3.2. Electronic properties

We begin our discussion with the electronic properties (i.e., band structure and total density of states (TDOS)) of pure HgTe. In Fig. 4, the band structure calculations indicate that HgTe behaves as a semimetal, characterized by the overlap between the conduction band maximum and the valence band minimum. It is worth recalling that a semimetal can be viewed as a semiconductor in which the lower energy states of the conduction band slightly overlap with the higher energy states of the valence band, although it is rarely described in these terms. The behavior of the band structure within this framework is consistent with previous studies.

The investigation of the band structure of undoped HgTe is essential as it provides critical information, such as the band gap. As shown in Fig. 4, the calculated band gap for HgTe is -0.16 eV. Although this value is smaller than the experimental value of -0.3 eV [26], it remains consistent with other values reported in the literature: -0.56 eV [25], -0.84 eV [27], and -0.15 eV [28].

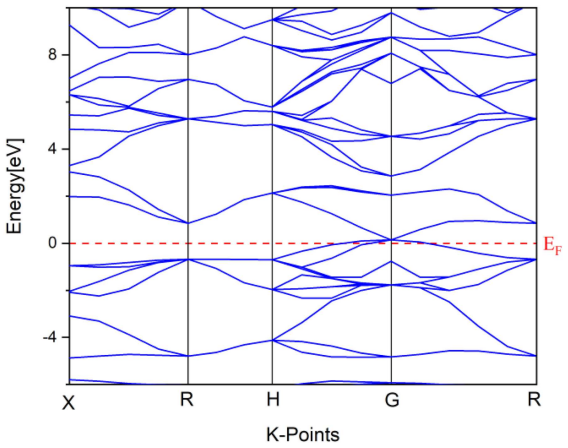

Fig. 4. Calculated band structure of the pure compound HgTe.

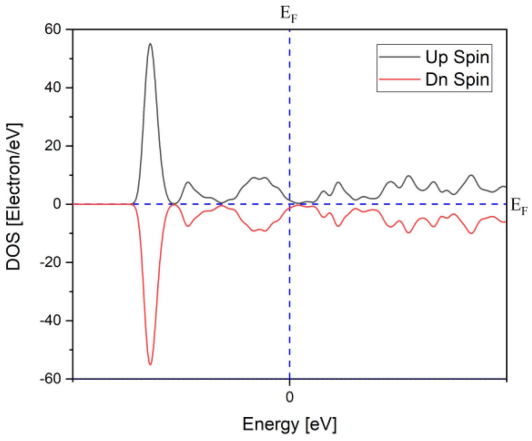

Fig. 5. TDOS of pure HgTe compound.

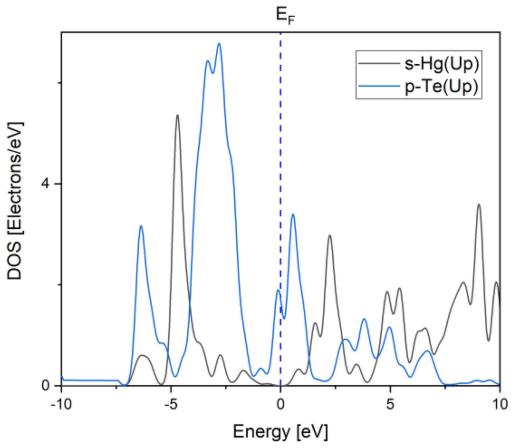

Fig. 6. PDOS of pure HgTe compound.

Figures 5 and 6 present the results of the total and partial density of states calculations, respectively. The valence band (VB) is separated into two distinct regions, while the conduction band (CB) forms a single continuous region, exhibiting strong symmetry between spin-up and spin-down states. These two bands are separated by a band gap (E_g) with a width of 0 eV. This analysis indicates that the HgTe compound is a non-magnetic semiconductor.

In addition, the perfect symmetry between spin-up and spin-down states confirms the absence of any magnetic behavior in HgTe. The total magnetic moment has been calculated to be 0 μ_B. Furthermore, the compound exhibits a zero band gap and a very small density of states at the Fermi level. These findings align with the previous analysis and confirm the semimetallic behavior in our system.

In our study, even for V concentrations below 12.5%, the majority spin channel remains metallic, while the minority channel exhibits a clear semiconducting character (see Fig. 7). Consequently, the system maintains a half-metallic nature, rather than becoming a full insulator, as reported by Cuono et al. [29]. This discrepancy can be attributed to both the doping concentration investigated in our work and the exchange-correlation approximation employed.

It is well known that the GGA+U approach introduces a corrective potential that significantly affects systems containing strongly correlated d electrons, such as transition metal ions. The inclusion of the U term lowers the energy of the occupied d states and shifts the unoccupied states upward, effectively widening the band gap in both spin channels. As a result, calculations using GGA+U+SOC may predict an insulating behavior, while standard GGA, which often underestimates the on-site Coulomb interaction, can yield a metallic or half-metallic phase. Therefore, our results are consistent with Cuono et al. [29] once the Hubbard correction is considered.

The choice of a 12.5% vanadium concentration in our work was motivated by the following considerations:

- Our primary objective was to demonstrate the existence of half-metallic behavior, 100% spin polarization, and to examine the ferromagnetic nature acquired after V doping in HgTe.
- At a V concentration of $x = 12.5\%$, the system exhibits a ferromagnetic ground state and higher spin polarization than at other concentrations; these two features are crucial for spintronic applications.
- At lower concentrations ($x < 12.5\%$), we observed magnetic instability and spin disorder, which can be explained by variations in exchange coupling constants, which determine the type of magnetic interactions between V atoms.
- Other dopants, such as Mn and Co, although displaying high spin polarization, exhibit neither half-metallicity nor ferromagnetic stability. Hence, V-doped HgTe at 12.5% remains the most promising configuration for achieving efficient spintronic behavior.

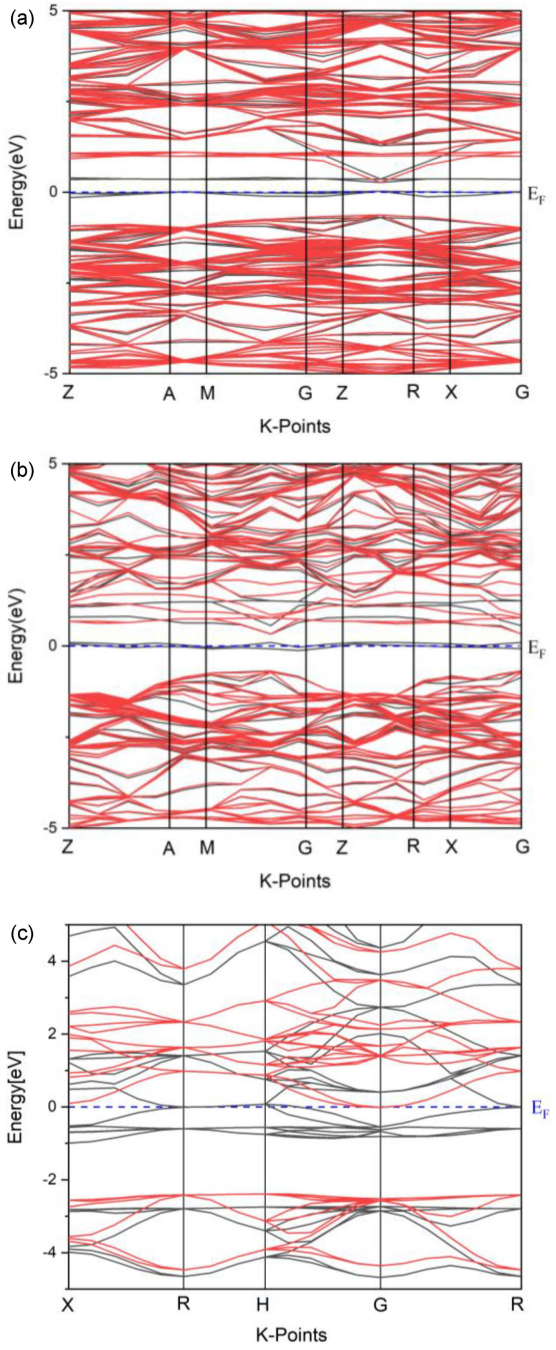

Fig. 7. Band structures of $Hg_{1-x}V_xTe$, where (a) $x = 3.125\%$, (b) $x = 6.25\%$, (c) $x = 12.5\%$.

Therefore, for the investigation of the other properties of $Hg_{1-x}V_xTe$, only the 12.5% dopant concentration will be considered.

To break the symmetry between major and minor spins and to induce magnetic behavior in the HgTe compound, we introduced vanadium (V) — a transition metal — into its structure. The results obtained are shown in Figs. 8–10. The introduction of V into the HgTe compound leads to significant changes in the band gap compared to the undoped material, particularly in the band gaps of the spin

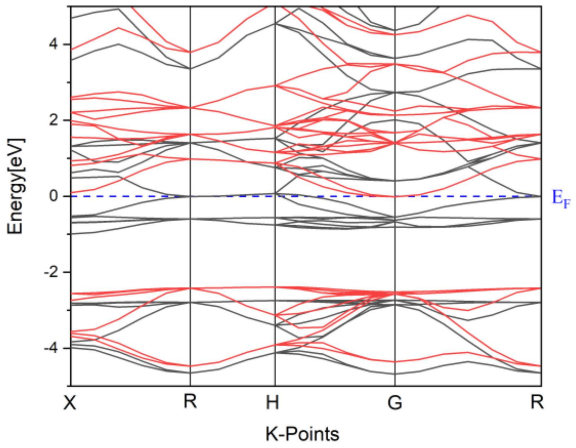

Fig. 8. Calculated band structure of V-doped HgTe. The Fermi level (E_F) is represented by the dashed line, with majority-spin (black line) and minority-spin (red line).

channels. In the spin-down channel, the band gap increases due to the additional electrons introduced by the V atoms, which occupy electronic states and push them away from the Fermi level, resulting in a widening of the gap. On the other hand, in the spin-up channel, the band gap decreases as the valence band shifts upward due to the presence of V impurities. This shift brings the valence band closer to the conduction band, thereby narrowing the gap. These changes are clearly illustrated in Fig. 8. The presence of distinct band gaps in the two spin channels makes $Hg_{1-x}V_xTe$ a highly promising material for spintronic applications. In spintronics, the ability to control and manipulate electron spin is essential, and materials with spin-selective band gaps can significantly enhance the performance and functionality of spin-based devices.

Figure 9 presents TDOS for the $Hg_{1-x}V_xTe$ compound with a vanadium doping concentration of $x = 12.5\%$. The system exhibits semimetallic properties accompanied by a magnetic behavior. This result is confirmed in Fig. 10, which presents the partial density of state (PDOS) for the doped compound, highlighting the contribution of vanadium dopant, particularly its $3d$ orbitals, and the strong hybridization observed between the Te-p and V-$3d$ orbitals. Analysing the energy levels reveals that the d orbitals are split into two energy levels, i.e., e and t_2. The e^+ orbit is fully filled, while the t_2^+ orbit is partially filled. Meanwhile, the e^- and t_2^- orbits remain empty. This is consistent with results reported in the literature [30].

Figure 10 shows the PDOS for HgTe doped with a single V impurity. The bandgap (E_g) values, spanning from 0.9 to 3.1 eV, originate primarily from the V-$3d$ states, with a minor contribution from the Te-p states observed in both spin channels. These results highlight that the introduction of V modifies the electronic structure of HgTe and that

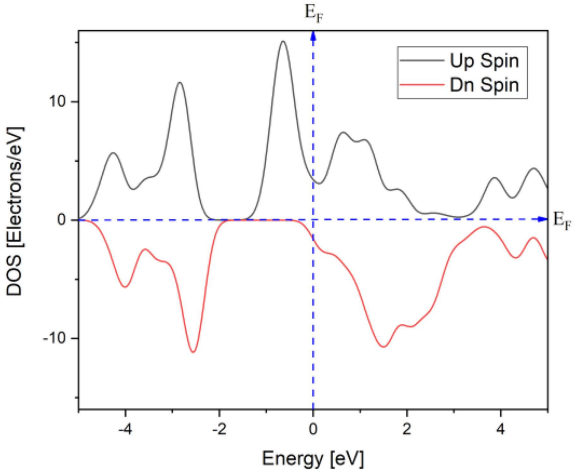

Fig. 9. TDOS of V-doped HgTe.

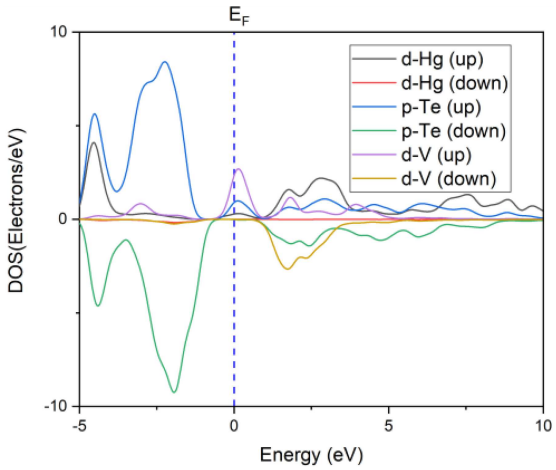

Fig. 10. PDOS of V-doped HgTe.

an analysis of the PDOS for $Hg_{1-x}V_xTe$ provides significant insights. (Recall that the electron configurations of tellurium (Te) and vanadium (V) are [Ar] $4d^2 5s^2 5p^4$ and [Ar] $3d^5 4s^2$, respectively.)

The data shown in Fig. 10 indicate a clear covalent bond between V and Te atoms, arising from the *p–d* hybridization near the Fermi level. These findings are consistent with the expected behavior of transition-metal-doped HgTe systems and align with previous studies [31]. The observed *p–d* hybridization is crucial for understanding the electronic interactions within the doped material, emphasizing the role of vanadium in modifying the electronic structure of HgTe. This modification imparts distinctive electronic and magnetic properties, making the material suitable for a range of advanced applications. For example, $Hg_{1-x}V_xTe$ could be valuable in magnetic electronics, enabling better control over electron spin, which is very useful for memory and logic devices. Its optoelectronic properties could also enhance performance in infrared detectors and solar panels due to specific

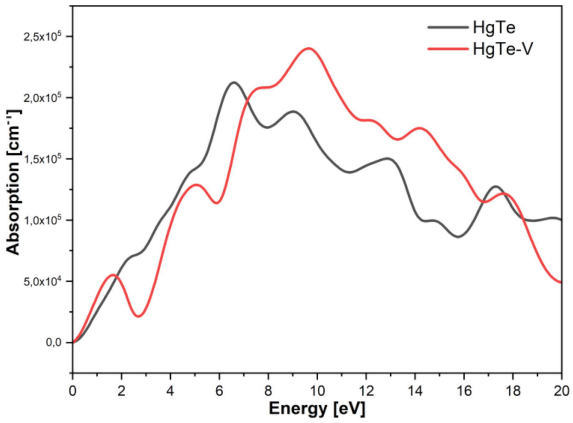

Fig. 11. Absorption spectrum of pure HgTe and V-doped HgTe.

interactions near the Fermi level. Finally, combining the semiconducting and magnetic properties of $Hg_{1-x}V_xTe$ could lead to the development of more advanced magnetic sensors and other innovative devices for future electronics.

3.3. Optical properties

To investigate the influence of vanadium (V) doping on the optical properties of HgTe, we analyze key parameters within the linear response regime, including the dielectric function, absorption coefficient, reflectivity, and energy loss function. The results are presented below, with the detailed derivation process available in [32]. This analysis follows the framework of direct transition probabilities and the Kramers–Kronig relations

$$\varepsilon(\omega) = \varepsilon_1(\omega) + \mathrm{i}\varepsilon_2(\omega), \tag{2}$$

where $\varepsilon_1(\omega)$ and $\varepsilon_2(\omega)$ are, respectively, the real and imaginary parts of the dielectric function as a function of the optical frequency ω.

3.3.1. Absorption spectrum

The optical absorption coefficient $\alpha(E)$ as a function of photon energy E [eV] can be expressed by

$$\alpha(E) = \frac{2E}{\hbar c}\sqrt{\frac{\sqrt{\varepsilon_1^2(\omega)+\varepsilon_2^2(\omega)}-\varepsilon_1(\omega)}{2}}, \tag{3}$$

where $\hbar$ and c represent the Planck constant and the speed of light in vacuum, respectively.

As shown in Fig. 11, the absorption coefficient α is approximately 10^5 cm^{-1}. The absorption border of the pure compound is located around 2.5 eV, indicating that it is a material with interesting optical properties. Optical absorption increases as photon energy rises. The injection of carriers by the dopant

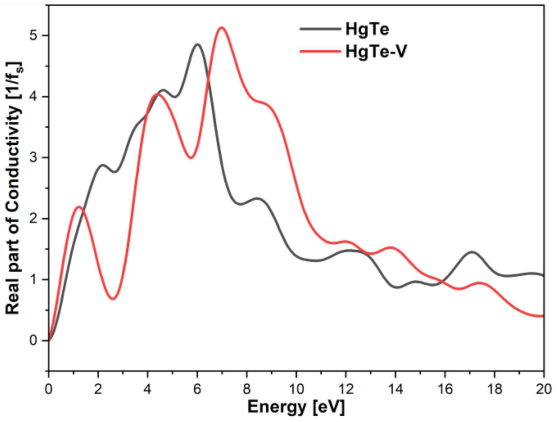

Fig. 12. Real part of the conductivity of HgTe and V-doped HgTe.

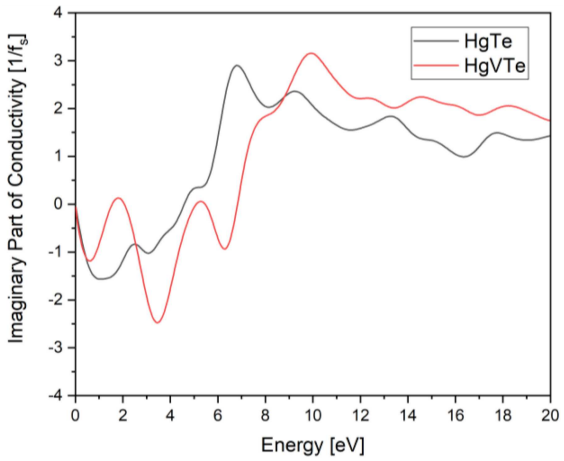

Fig. 13. Imaginary part of the conductivity of HgTe and V-doped HgTe.

element V induces a shift, which is observed as the absorption edge of the doped compound moves toward higher energy.

3.3.2. Conductivity

The optical conductivity $\sigma(\omega)$ characterizes the conductivity of photoelectrons generated by the photoelectric effect within a material. It can be calculated using the following formula

$$\sigma(\omega) = \frac{\omega}{4\pi} \operatorname{Im}(\varepsilon(\omega)). \tag{4}$$

Figure 12 shows the conductivity curves. In the energy range from 4 to 8 eV, both systems exhibit high conductivity. This increase is proportional to the energy of the incident photons in the visible region. The maximum peak is observed at 7 eV for the doped compound and at 6 eV for the pure compound, with corresponding values of 5.17 fs^{-1} and 4.72 fs^{-1}, respectively. These results indicate that V doping enhances the optical conductivity of HgTe in this spectral range. Despite this improvement, the overall conductivity of both systems remains relatively low. The negative conductivity observed in Fig. 13 does not indicate that the doped compound rejects current; rather, it reflects an unusual response potentially linked to particular physical effects such as the Hall resistance.

3.4. Magnetic properties

Table II presents the contribution of each element to the total and partial atomic magnetic moments [in μ_B] for the V-doped HgTe compound ($Hg_{1-x}V_xTe$).

It is evident from the table that the magnetism of the compound primarily originates from the impurity atom, i.e., vanadium (V). To confirm this,

TABLE II

Calculated magnetic moments given in [μ_B] for V-doped HgTe.

Hg	V	Te	Interstitial	Total
0.206	1.961	0.030	0.803	3

TABLE III

Polarization of V-doped HgTe as a function of V concentration.

Concentration of V [%]	Polarization
8	87.8%
12	89.4%
15	91.1%
20	91.5%
24	93.6%

the concentration of V was increased, and it was observed that both the total and partial magnetic moments increased proportionally with the V concentration (see Table III). Therefore, the positive and negative signs of the partial spin magnetic moments for each atom (Hg, V, and Te) indicate the direction of their respective moments. The electron spin polarization can be calculated using the following expression

$$P = \frac{\rho^{\uparrow} - \rho^{\downarrow}}{\rho^{\uparrow} + \rho^{\downarrow}}, \tag{5}$$

where:

- $\rho^{\uparrow}$ — majority spin states,
- $\rho^{\downarrow}$ — minority spin states.

The majority spin states of the V-3d orbitals are partially filled with three electrons, resulting in a total magnetic moment of $\approx 3\ \mu_B$. TDOS is primarily influenced by the V-3d and Te-p states, which are the main contributors to the overall

magnetic moment in $Hg_{0.875}V_{0.125}Te$. A strong p–d hybridization is observed between the Te-p and V-3d states in the majority spin channel, leading to a reduction in the system's total energy and confirming the ferromagnetic configuration of our compounds. This hybridization also induces small local magnetic moments on the non-magnetic Hg and Te atoms. Both Hg and Te exhibit parallel magnetic polarization, further indicating ferromagnetic behavior.

3.5. Curie temperature (T_C)

Since the approximation used only describes the properties of the ground state, an additional approach — such as the Heisenberg mean-field approximation — is needed to characterize the magnetic properties at finite temperature. In fact, a simple Heisenberg model allows one to estimate the Curie temperature, which is implemented in the SIESTA code. This model is expressed by

$$H = -\sum_{i \neq j} J_{ij}\ \boldsymbol{S}_i \cdot \boldsymbol{S}_j, \tag{6}$$

where:

- $\boldsymbol{S}_i$ — spin at site i,
- J_{ij} — exchange constant between sites i and j.

To estimate the Curie temperature, we apply the Weiss mean-field formula derived from the Hamiltonian (6), thus

$$T_C = \frac{2}{3k_B}\ S\,(S+1) \sum_i z_i J_i, \tag{7}$$

where:

- S — spin quantum number of the magnetic ion,
- z_i — coordination number (number of neighboring magnetic atoms) for the i-th shell,
- J_i — exchange interaction for the i-th neighbor,
- k_B — Boltzmann's constant.

The exchange interactions J_i can be derived from first-principles DFT total energy calculations by evaluating the energy difference between different magnetic configurations. Specifically, the effective exchange energy ΔE is defined as

$$\Delta E = E_{DLM} - E_{FM}, \tag{8}$$

where:

- E_{DLM} — energy of the disordered local moments (DLM) state,
- E_{FM} — energy of the ferromagnetic (FM) ground state.

Table IV presents the calculated energies of the ferromagnetic phases for each concentration.

TABLE IV

Total energy difference and ferromagnetic stability for each concentration.

Concentration	ΔE ($\times 10^{-3}$) [eV]	Ferromagnetic stability
8	4.33	stable
12	6.29	stable
15	7.48	stable
20	8.40	stable
24	9.86	stable

This total energy difference can be interpreted within the Heisenberg model as

$$\Delta E^H = S^2 C^2 \sum_{n \neq 0} J_{n0}, \tag{9}$$

where C represents the dopant concentration. The summation is running over all interacting magnetic neighbors in the sublattice.

By combining the energy difference ΔE obtained from DFT with the mean-field expression for T_C, we derive the following simplified practical formula [33]

$$T_C = \frac{2}{3}\ \frac{\Delta E}{C\,k_B}. \tag{10}$$

This equation provides a straightforward way to estimate the Curie temperature directly from first-principles calculations, incorporating both the magnetic energy and the dopant concentration. Using (10), we estimate the Curie temperature for the V-doped HgTe ferromagnetic compound to be 315 K. This value can be considered high at a relatively low doping concentration. Our findings are consistent with prior computational studies on diluted magnetic semiconductors (DMS) doped with transition metals such as Co and V [19, 34].

It is important to note, however, that the mean-field approximation tends to overestimate T_C, particularly at low dopant concentrations, because it neglects thermal spin fluctuations and disorder effects. Nevertheless, this approach remains a valuable and computationally efficient framework for predicting magnetic ordering temperatures in doped semiconductors from first principles.

4. Conclusions

This paper investigates the electronic and magnetic properties of $Hg_{1-x}V_xTe$ with $x = 0.125$, using density functional theory (DFT) with the Perdew–Burke–Ernzerhof (PBE) generalized gradient approximation (GGA) exchange-correlation functional. The results demonstrate the potential of V-doped HgTe as a stable ferromagnetic material. Specifically, we find that the $Hg_{0.875}V_{0.125}Te$ compound exhibits robust ferromagnetism with a high

spin polarization of 90%, driven by the ferromagnetic p–d exchange coupling mechanism.

The stability of the ferromagnetic phase is confirmed by positive total energy differences and the presence of antibonding states resulting from p–d hybridization, suggesting the onset of spontaneous magnetization. Furthermore, the significant p–d hybridization between the p orbitals of tellurium (Te) and the partially filled $3d$ orbitals of vanadium (V) in $Hg_{0.875}V_{0.125}Te$ leads to a reduction in the total magnetic moment of the V atom from its free-space value of 3 μ_B. This interaction also induces small local magnetic moments on the nonmagnetic Hg and Te sites.

The electronic structure of $Hg_{0.875}V_{0.125}Te$ exhibits a diverse gap character, enhancing its potential as a candidate material for spin injection applications in spintronic devices. The ability to control and manipulate spin states in such materials holds significant promise for advancing technologies based on spin polarization and magnetic behaviors.

References

[1] M.E.A. Monir, H. Baltache, G. Murtaza, R. Khenata, W.K. Ahmed, A. Bouhemadou, T. Seddik, *J. Magn. Magn. Mater.* **374**, 50 (2015).

[2] M. Kurpas, B. Kędzierska, I. Janus-Zygmunt, M.M. Maśka, E. Zipper, *Acta Phys. Pol. A* **126**, A20 (2014).

[3] M.H.F. Sluiter, Y. Kawazoe, P. Sharma, A. Inoue, A.R. Raju, C. Rout, U.V. Waghmare, *Phys. Rev. Lett.* **94**, 187204 (2005).

[4] T. Dietl, H. Ohno, F. Matsukura, J. Cibert, D. Ferrand, *Science* **287**, 1019 (2000).

[5] V.K. Sharma, R. Xalxo, G.D. Varma, *Cryst. Res. Technol.* **42**, 34 (2007).

[6] S. Wolski, C. Jasiukiewicz, V. K. Dugaev, J. Barnaś, T. Slobodskyy, W. Hansen, *Acta Phys. Pol. A* **127**, 472 (2015).

[7] A. Zitouni, S. Bentata, W. Benstaali, B. Abbar, *Solid State Commun.* **190**, 40 (2014).

[8] A.S. Jbara, M.A. Saeed, M.U. Saleem, *Optik* **179**, 1118 (2019).

[9] N.A. Noor, S.M. Alay-e-Abbas, Y. Saeed, S.M. Ghulam Abbas, A. Shaukat, *J. Magn. Magn. Mater.* **339**, 11 (2013).

[10] M. Sedlmayr, N. Sedlmayr, V.K. Dugaev, *Acta Phys. Pol. A* **135**, 1268 (2019).

[11] A. Waag, F. Fischer, H.J. Lugauer et al., *J. Appl. Phys.* **80**, 792 (1996).

[12] J. Li, X. Xu, Y. Zhou, M. Zhang, X. Luo, *J. Alloys Compd.* **575**, 190 (2013).

[13] K. Viloane, M.G. Sreenivasan, K.L. Teo, T. Liew, T.C. Chong, *J. Appl. Phys.* **99**, 08D514 (2006).

[14] B.K. Roberts, A.B. Pakhomov, K.M. Krishnan, *J. Appl. Phys.* **103**, 07D133 (2008).

[15] A. Labrag, M. Bghour, E. Salmani, F. Goumrhar, H. Ez-Zahraouy, *Indian J. Phys.* **96**, 4193 (2022).

[16] M. Baiboud, A. Labrag, M. Bghour, M. Khenfouch, H. Charkaoui, A. Abou El Hassan, H. El Ouaddi, S. Laasri, *Eur. Phys. J. Appl. Phys.* **99**, 15 (2024).

[17] C. Śliwa, C. Autieri, J.A. Majewski, T. Dietl, *Phys. Rev. B* **104**, L220404 (2021).

[18] C. Autieri, C. Śliwa, R. Islam, G. Cuono, T. Dietl, *Phys. Rev. B* **103**, 115209 (2021).

[19] K. Sato, P.H. Dederics, H. Katayama-Yoshida, *Europhys. Lett.* **61**, 403 (2003).

[20] T. Skauli, T. Colin, *J. Cryst. Growth* **222**, 719 (2001).

[21] F. Birch, *Phys. Rev.* **71**, 809 (1947).

[22] A. Svane, N.E. Christensen, M. Cardona, A.N. Chantis, M. van Schilfgaarde, T. Kotani, *Phys. Rev. B* **84**, 205205 (2011).

[23] V.P.S. Perera, M.K.I. Senevirathna, P. Pitigala, K. Tennakone, *Sol. Energy Mater. Sol. Cells* **86**, 443 (2005).

[24] A. Hao, X. Yang, R. Yu, C. Gao, Y. Han, R. Liu, Y. Tian, *J. Phys. Chem. Solids* **70**, 433 (2009).

[25] B. Al Shafaay, F. El Haj Hassan, M. Korek, *Comput. Mater. Sci.* **83**, 107 (2014).

[26] R. Miloua, Z. Kebbab, F. Miloua, N. Benramdane, *Phys. Lett. A* **372**, 1910 (2008).

[27] X. Chen, A. Mintz, J. Hu, X. Hua, J. Zinck, *J. Vac. Sci. Technol. B* **13**, 1715 (1995).

[28] S. Adachi, *Properties of Group-IV, III-V, and II-VI Semiconductors*, Wiley, Chichester 2005.

[29] G. Cuono, C. Autieri, T. Dietl, *Phys. Rev. B* **110**, 165112 (2024).

[30] J.W. Allen, G. Lucovsky, J.C. Mikkelsen Jr., *Solid State Commun.* **24**, 367 (1977).

[31] Y. Harrache, N. Bouarissa, *Solid State Commun.* **295**, 26 (2019).

[32] K. Huang, *Solid State Physics*, Higher Education Press, Beijing 2002.

[33] K. Sato, H. Katayama-Yoshida, *J. Non-Cryst. Solids* **358**, 2377 (2012).

[34] M. Baiboud, A. Labrag, M. Khenfouch, M. Bghour, A. Tirbiyine, J. El Qars, H. Charkaoui, A. Chouchna, K. Elgoumiri, *J. Magn. Magn. Mater.* **627**, 173112 (2025).